Studies in thin diffraction gratings for flight applications

Ann Shipley, Brian Gleeson, Randall McEntaffer, Webster Cash

Ann Shipley, Brian Gleeson, Randall McEntaffer, Webster Cash, "Studies in thin diffraction gratings for flight applications," Proc. SPIE 6273, Optomechanical Technologies for Astronomy, 62733K (6 July 2006); doi: 10.1117/12.672288

SPIE.

Event: SPIE Astronomical Telescopes + Instrumentation, 2006, Orlando, Florida , United States

Studies in Thin Diffraction Gratings for Flight Applications

Ann Shipley, Brian Gleeson, Randall McEntaffer, and Webster Cash
University of Colorado, Center for Astrophysics and Space Astronomy, 593 UCB,
1255 38th St, Boulder, CO 80303-0593

ABSTRACT

The quest for maximum throughput in high energy astronomy instruments has influenced an increasing trend in spectrograph design toward closely packed mirror and grating arrays. Gratings have additional challenges to those required for mirrors and are evaluated separately in this study. Since these instruments typically operate above earth's atmosphere, grating arrays are subject to a launch vehicle environment. Packing gratings close together in a confined space decreases substrate thickness below traditionally accepted standards for maintenance of surface figure. The ever-present pressure to minimize mass in flight payloads drives substrates even thinner. The University of Colorado has performed a study of several methods that may be employed to make thin gratings. In this paper, some traditional techniques are compared to less conventional ideas for using thin substrates. Environmental effects necessary for flight applications are also folded into the analysis for each thin grating type.

Keywords: array, diffraction grating, electroform, foil, grating, off-plane mount, replica, thin substrate, x-ray

INTRODUCTION

1. Maximizing throughput and the off-plane mount

The desire to maximize throughput is common among optical designs across the electromagnetic spectrum. Gratings for high energy applications are typically mounted at grazing incidence for better reflectivity, but at the price of reduced active area and vignetting from adjacent gratings. An obvious solution to regain throughput and minimize shadows is to reduce the substrate thickness so that gratings may be packed closer together in an array. Although this method provides improvement, such a grating array used in a traditional in-plane mount will still suffer some vignetting of reflected orders. Following the next logical step brings us to the off-plane grating mount. The off-plane mount at grazing incidence brings light onto the grating at a low graze angle, quasi-parallel to the direction of the grooves. The light is then diffracted through an arc forming a cone, known as conical diffraction.[1, 2, 3]

The off-plane mount is a natural geometry for grazing incidence reflection gratings, and comes with a substantial set of advantages.[4] Clever designs can take advantage of its potential for higher resolution by employing higher dispersion designs and relaxed tolerances. Another advantage of the off-plane mount is diffraction efficiency. The effective diffraction efficiency of the off-plane mount can be substantially higher than traditional mounts (often a factor of two) due to the groove illumination function[5, 6]. Off-plane mounts do, however, require higher groove densities. Radial groove structure and blaze are also common tools used to improve performance. Therefore, this study compares reflection grating types based on off-plane criteria.

1.1. Common environmental considerations for spaceflight optics

Spaceflight optical systems are subject to various special environmental conditions imposed by a mission's orbit, altitude, and launch vehicle. Vacuum and gravity release are a given in applications above earth's atmosphere. Low outgassing materials should be used in optics and mounts to avoid molecular contamination, delamination, degradation, or possible sticking in mechanisms. Closed cavities such as those in honeycomb structures need to be vented to prevent distortion and delamination. Friction tends to increase in vacuum and galvanic attack must be considered at mating interfaces. Corrosion in flight designs is often overlooked, but exists in the form of pitting, stress-corrosion cracking, and hydrogen embrittlement in certain materials. Gravity is present during optic fabrication and alignment, but is released on-orbit resulting in optical surface figure and alignment variations.

Vibration and launch loads make high system stiffness and resonant frequency imperative in order to minimize dynamic response. Launch vehicles also have a limited envelope which the payload may not impinge upon. Components that are low in mass are desirable because they are less susceptible to excessive gravity loads during launch and vibration testing. Brittle materials often used for optics may be vulnerable to fracture under vibration and launch. Vibration may also be present on-orbit in the form of transmitted jitter that can result in mechanical instability.

Optomechanical Technologies for Astronomy, edited by Eli Atad-Ettedgui, Joseph Antebi, Dietrich Lemke,
Proc. of SPIE Vol. 6273, 62733K, (2006) · 0277-786X/06/$15 · doi: 10.1117/12.672288

Thermal conditions are highly variable with regard to a given mission. Thermal radiation is dominant in vacuum and must be considered when evaluating an optical system's performance on-orbit. Although most optical systems can be contained and temperature controlled within a satellite, temperature extremes between the sun and shade sections on the outside can be severe. Optical benches or structures can be susceptible to thermal stress or strain that can affect optical system alignment. Thermal excursions can also fatigue materials and coatings over the mission life and result in particulate contamination.

Depending on orbit, altitude, and system design, materials may also be exposed to charged particle radiation, atomic particle degradation, micrometeroids, and orbital debris. Optical systems for spaceflight applications should be designed to operate throughout the expected mission lifetime. Careful material choices based on the expected on-orbit environment are always a good idea.

ELECTROFORMED NICKEL GRATINGS

2. Performance Requirements

The Cygnus X-ray Emission Spectroscopic Survey (CyXESS) is a University of Colorado sounding rocket payload scheduled to launch from White Sands Missile Range in spring 2006. The optical instrument is contained in a ∅22 inch rocket skin that includes up to six densely packed off-plane grating arrays.[4, 7, 8]

An array consists of 67 gratings mounted 1.5mm apart at a 4.4º graze angle. Each replicated grating is rectangular in shape with 104mm x 20mm active area and 0.127μm thick. Instrument performance dictates that each mounted grating is restricted to a maximum allowable slope error that differs for the two ordinate directions on the grating surface. This slope error is the sum of the grating surface error (see figure 2) and the grating alignment error (grating parallelism). The total allowable error is 30 arcminutes perpendicular to the grooves (along 104mm length) and 2.5 degrees parallel to the grooves. An equivalent flatness requirement translates to about 0.5mm with some additional restrictions in the frequency of errors over the grating surface. See figure 1. These constraints were arrived at by first determining the maximum allowable spectral line width on the rocket's detector plane and from this calculating the maximum grating slope that would produce such a line.

These gratings are used in an off-plane mount and have a replicated sinusoidal groove density of 5670 grooves/mm. Grating grooves are parallel in structure and extend across the 20mm width of the grating. The optical design for this system purposefully limits the grating groove length so that a radial groove structure is not necessary to obtain the desired resolution of 100 ($\lambda/\Delta\lambda$). Measured groove efficiency of first and second diffracted orders in these gratings is about 32% at Carbon 0.277keV with a 4.4º graze angle.

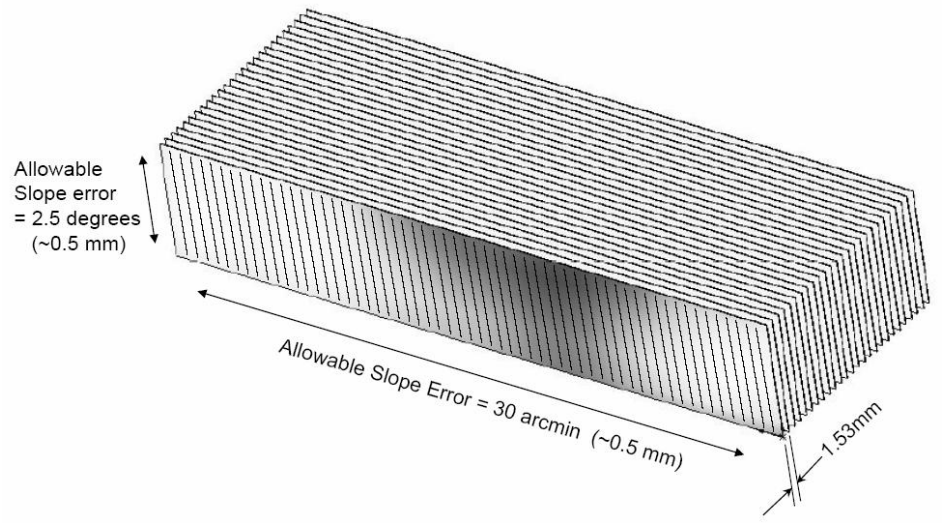

Figure 1. Allowable slope error

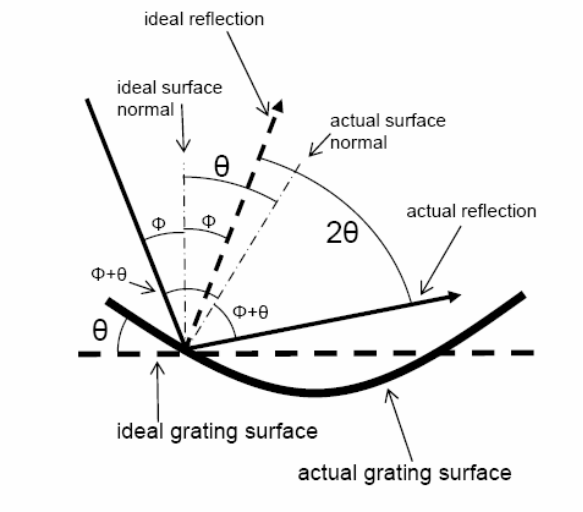

Figure 2. Angular surface error, θ

2.1. Grating fabrication

Budget limitations often play a large role in sub-orbital rocket design. In this case, the least expensive method of producing several hundred foil grating substrates naturally led to electroformed nickel (EF). Sheets of 0.005 ± 0.0003 inches thickness are deposited onto a flat polished mandrel. Each sheet is large enough to make five separate grating substrates. Table 1 lists some measured mechanical properties of electroformed nickel.

Table 1. Electroformed Nickel Material Properties

Tensile Strength	147,000 psi	1.0 GPa
Elastic Modulus	24e6 psi	165.5 GPa
Density	0.32 lb/in^3	8.91 g/cm^3
CTE, (α)	7.2 x 10^{-6} /ºF	13.0 x 10^{-6} /ºC

Good off-plane grating performance requires high groove density, and minimizing cost is imperative for this mission. Therefore, the grating groove profile is replicated from an existing master onto each electroformed substrate. The replication layer shrinks as the polymer cures resulting in bi-metallic bending of the thin substrate. This distortion is difficult to measure with any accuracy due to EF nickel's poor specific stiffness. However, the resulting curvature of an unrestrained substrate can be estimated using the following equation: [9]

$$\delta_{\Delta T} := \frac{r^2}{2}\cdot\left[\frac{3}{h}\cdot\frac{\psi_p}{\psi_m}\cdot\left(\alpha_p-\alpha_m\right)\cdot\Delta T\cdot\frac{h_{p1}-h_{p2}}{2\cdot h}\cdot\left[1-\frac{h_{p2}-h_{p1}}{2\cdot h}\cdot\left(4\cdot\frac{\psi_p}{\psi_m}-1\right)\right]\right] \quad (1)$$

where: $\delta\Delta T$ = *is the change is mirror optical surface radius*
r = *mirror radius (geometry)*
$2h$ = *mirror thickness, along optical axis*
h_p = *plating thickness (1 for mirror front, 2 for back)*
ΔT = *change in temperature*
α = *thermal coefficient of expansion*
ψ = *stiffness parameter*
E = *elastic modulus*
ν = *Poisson's ratio*

Volumetric shrink rate for the replication polymer can be represented as temperature change in the following way:

$$\Delta T := \frac{1 - \sqrt[3]{1 - p}}{\alpha_p} \tag{2}$$

where: ΔT *= equivalent change in temperature*
p *= polymer shrink percentage by volume (i.e 0.002)*
α_p *=polymer thermal coefficient of expansion*

Given the poor structural efficiency of the substrate material and its extreme thinness, surface distortion due to replication layer cure shrinkage is estimated at 120μm. The resulting sag over half the length of the substrate translates to about 457arcseconds. Since the substrate is very pliable, this curvature is easily corrected when the grating is secured in its mount. A thin coating of electroless nickel is used as a reflective layer in order to match material thermal expansion coefficients and minimize potential bi-metallic bending due to thermal changes. The sheet is then divided into five gratings of final dimension using femtosecond pulsed lasers that cut through the epoxy replication layer without raising its temperature.

2.2. Mount and environmental analysis

The choice of electroformed nickel as a substrate offers an inexpensive way to fabricate a large quantity of nearly identical thin substrates and provides the luxury of a material not prone to fracture under launch and vibration testing. However, thin electroformed nickel is not particularly stiff in relation to its mass and deflects easily under small loads. Low outgassing replication epoxy is used to minimize possible delamination during flight and vacuum testing. Gravity presents several challenges when working with very thin EF nickel substrates. Although the substrate deflection is minimal on edge, deflection due to gravity increases substantially as its orientation moves off edge. Figure 3 and Table 2 show finite element analysis results for a grating clamped at each end that is subjected to 1g perpendicular to the grating active surface, on edge, and in its alignment orientation (on edge at graze angle).

Table 2 Grating FEM displacement in gravity

Gravity load	Grating Deflection, μm
1g in Z (shown here)	282
1g in Y	0.02
1g 4.4º from Y	17

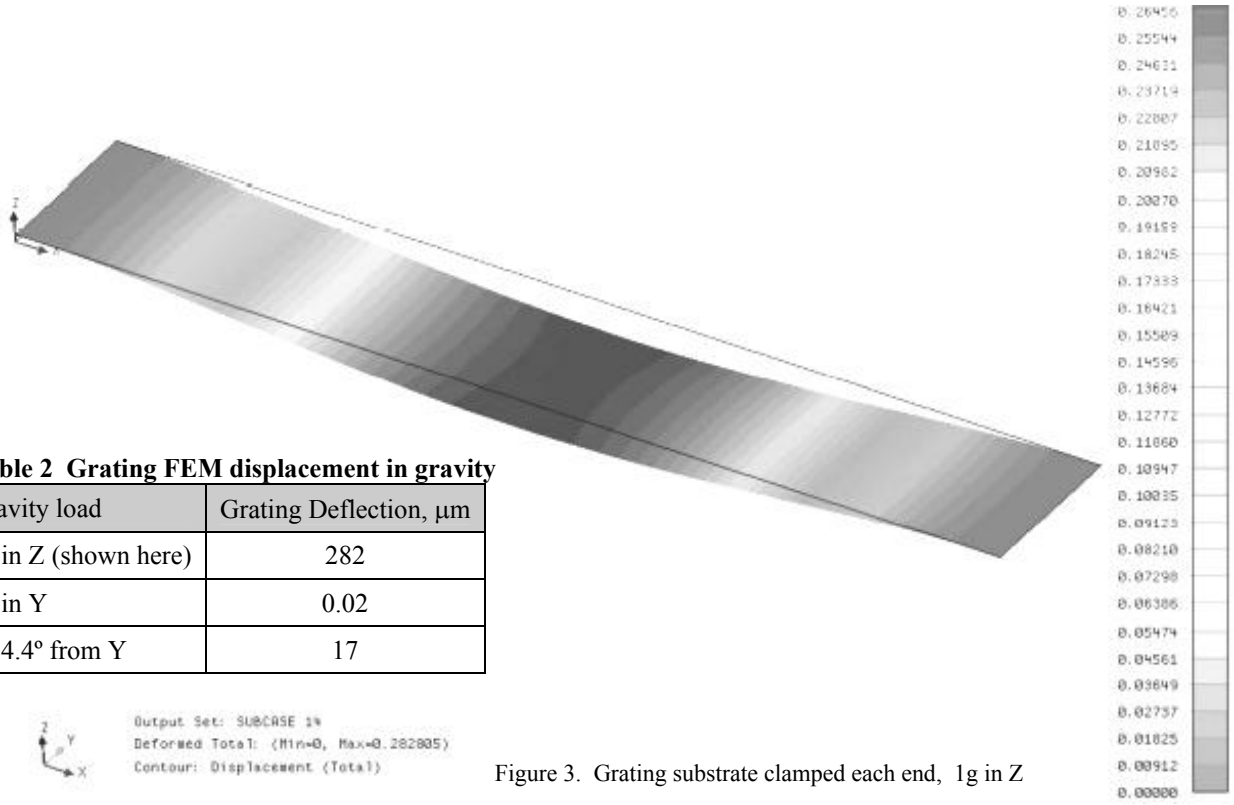

Figure 3. Grating substrate clamped each end, 1g in Z

The grating is also subject to dynamic response under vibration tests and during launch. Excessive bending due to response needs to be minimized to prevent possible peel at grating edges or collision between adjacent gratings in the array. A static equivalent launch load can be estimated from the rocket's random vibration test profile using Miles' Approximation.[10]

$$g_{rms} \approx \sqrt{\frac{\pi}{2} \cdot f_n \cdot Q \cdot PSD} \tag{3}$$

where: f_n = *fundamental frequency (Hz)*
Q = *resonant amplification*
PSD = power spectral density (g^2/*Hz*)

The grating's maximum displacement response is a function of fundamental frequency and the equivalent launch load.[10]

$$\delta = \frac{g_{rms}}{(2\pi \cdot f_n)^2} \tag{4}$$

w*here:* δ = *maximum displacement response*
g_{rms} = *root-mean-square acceleration*
f_n = *fundamental frequency*

An eigenvalue analysis of a grating substrate clamped at each end is used to predict fundamental frequency and a first order beam bending mode shape. In order to reduce bending deflection the substrate's fundamental frequency is raised by pulling it into tension. Table 3 shows predicted displacements for a grating held at increasing levels of tension. Since most structural damage in flight structures occurs at 3σ load levels, the gratings will be held at 18-22N to prevent collision of adjacent gratings that may oscillate out of phase.

Table 3. Clamped grating substrate in tension

Load case	fn (Hz)	grms	$\delta@g_{rms}$ (m)	$\delta@g_{3\sigma}$ (m)
No tension	34	4	8.6 x 10-4	2.5 x 10-3
4.5N tension	68	7	3.5 x 10-4	1.1 x 10-3
18N tension	120	13	2.24 x 10-4	6.72 x 10-4
22N tension	133	16	2.22 x 10-4	6.67 x 10-4

A grating array is held in a titanium flexure mount designed to pull each of the 67 gratings into 22N (5lbf) tension.[11] Figure 4 shows a full complement of gratings assembled into the flexure mount. Gratings are aligned in precision slots with their corners exposed on the front and back side of the mount by counterbored sections. An alignment/bonding fixture is used to pin the flexure in a fully displaced position (0.25mm) during assembly and alignment of the gratings. The counterbores are then filled with epoxy to bond the gratings in place. Upon completion of the cure cycle, the flexure is released to pull gratings into tension. Eigenvalue results predict the flexure fundamental frequency at 961 Hz with first order beam bending of the flexure block in its designed displacement direction. Dynamic deflection of the flexure under launch is estimated at 33μm, which is a small fraction of the total flexure displacement, and allows gratings to remain in tension even at resonance.

An engineering unit was built with three pairs of EF gratings mounted at the left, right, and center of the flexure to demonstrate alignment across the array. The measured gratings had a maximum surface error of 15 arcminutes and a grating parallelism error of 12 arcminutes, for a total slope error of 27 arcminutes. This is within the maximum allowable slope error of 30 arcminutes. The flight gratings are expected to have even better flatness due to an improved laser cutting process. Flight mounts are currently being fabricated and are expected to exceed performance requirements for this system.

Sub-orbital rocket flights only spend several minutes above earth's atmosphere and are not susceptible to longer term conditions such as radiation, atomic particles or orbiting projectiles. Primary environmental concerns are vacuum, gravity, vibration due to launch, and landing. Vacuum compatible material selection and venting practices are used to control possible molecular contamination, and to maintain mechanical stability and alignment. Thermal conditions depend on optical design and sensitivity. This instrument is designed to perform adequately under expected ambient thermal conditions during the flight. Resonance, dynamic deflection, and gravitational effects have also been addressed in the system design. The mounted EF nickel gratings are robust in a vibration environment and not susceptible to fracture, but their stability over time under tension is unknown. Anomalies to watch for over time include possible optical surface changes due to creep, stress relaxation, and stress corrosion cracking.

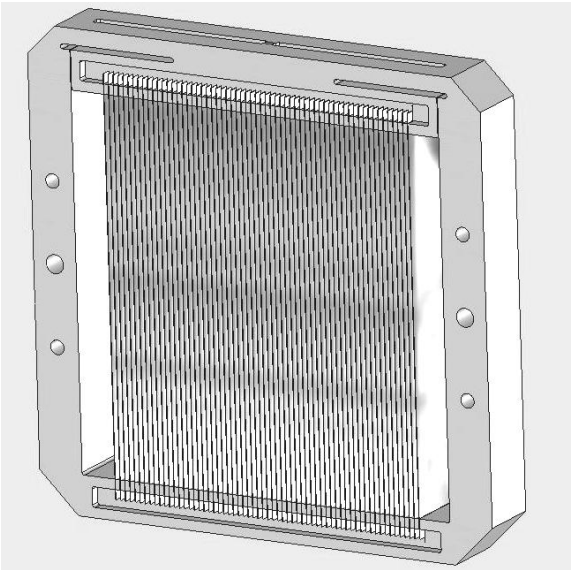

Figure 4. CyXESS Grating Mount Assembly

CONVENTIONAL REPLICATION ONTO THIN SUBSTRATES

3. Replication cure and gravitational effects

Conventional replication for diffraction gratings using low-outgassing polymers is well established for flight applications. The University of Colorado has worked with Horiba Jobin-Yvon (JY) for over a decade to produce replicated flight gratings for both in-plane and off-plane mounts. Many of these gratings have high line-density holographically recorded grooves used for aberration control on missions such as FUSE and COS.[12, 13, 14, 15] Holographic recording techniques have also been used to produce high density radial groove patterns.[16] Grating performance can be further enhanced by adding blaze to these types of profiles using ion etching. Diffraction efficiency for sinusoidal un-blazed gratings in the off-plane mount is measured at ~35-45% in the soft x-ray range. Some in-plane scattering has been observed for ion-etched gratings used in the off-plane configuration. This is considered a soluble issue and efficiencies are expected to improve when it is corrected. Since the majority of challenges needed to meet our stated performance requirements have already been demonstrated using these techniques, it makes sense to transfer that technology to a thin substrate application.

Conventional replication methods were developed using a traditional substrate thickness of about 1/6 the diameter of a circular optic. Therefore, the challenge lies in exploring how conventional methods affect replication onto a thin substrate. Replication polymers shrink as they cure through outgassing of solvents, catalysts, and curing agents. Shrink rates vary with each type of resin and are generally represented as a percentage by volume. In optics of traditional thickness this shrinkage typically has such a negligible effect on surface figure that it is ignored. However, in thin substrates it results in bi-metallic bending whose magnitude depends upon the optic's geometric shape, material properties, and replication layer thickness.

JY produced replicas on Pyrex flats of size 100mm x 100mm x 2mm (ground flat to ~$\lambda/4$) using low-outgassing resin, and standard tooling. Measured surface figure of the replicas were distorted up to 10 waves or 6.3

microns, which matches the analytical estimate shown in Table 4. Next, a flat was replicated on both the front and back sides, but it resulted in no significant improvement over the one-sided replication. Several factors from the standard replication process contribute to excessive distortion observed in these thin Pyrex replicas. First, the tooling and process used for thick substrate replicas allows the resin layer to vary from about 30-50 microns in thickness. Another contributing problem is wedge shaped variation in the resin thickness across the length and width of the replication layer. Also, although Pyrex may be ground quite flat, it does not have good mechanical stiffness making it vulnerable to bending. Results of the tests show that bi-metallic stress is dominant in these thin substrates despite their flatness prior to replication.

Another test was performed using much stiffer silicon carbide CVD substrates, also 2mm thick, but with loosely controlled surface flatness to reduce cost. Distortion in the replicas for these tests greatly exceeds predicted bi-metallic bending using equations 1 and 2 in the previous section. It is likely that there is residual stress in these inexpensively produced substrates along with test setup error due to gravity that masks the effect we are trying to quantify. We performed finite element analysis on rectangular substrates of different thickness restrained in identical optimized five point mounts to predict surface error in gravity, see figure 6(a). The plot in Figure 7(a) shows results for a similar analysis on a ∅100mm silicon wafer. Table 4 shows predictions for displacements of substrate surfaces perpendicular to gravity, on edge, and tilted one degree off edge. The relationship between replication layer thickness and bi-metallic bending was calculated using equations 1 and 2, also shown in Table 4. Surface error is plotted as a function of replica layer thickness in materials of equivalent size and thickness in Figure 5 to illustrate the importance of substrate stiffness. Materials with higher specific stiffness can tolerate a thicker replication layer for a given allowable surface error.

Table 4 Conventional replication cure and gravitational effects on substrates

Substrate Type (100mm x 100mm) (r = 70.7mm)	Substrate Thickness (mm)	Replica layer (μm)	Areal density (g/cm^2)	Bimetallic Bending (arcsec)	Bimetallic Bending (m)	Displacement (m)		
						1g in Z	1g in Y	1g @1°off Y
Pyrex	16.7	50	3.72	0.38	9.1e-8	3.6e-8	2.7e-9	2.7e-9
Pyrex	2.0	50	0.446	26	6.3e-6	1.6e-6	2.1e-9	1.4e-8
Pyrex	2.0	30	0.446	15	3.8e-6	1.6e-6	2.1e-9	1.4e-8
Pyrex	0.5	0.10	0.112	0.84	2.0e-7	2.5e-5	2.1e-9	2.1e-7
SiC CVD	2.0	50	0.642	3.41	8.3e-7	3.2e-7	4.1e-10	2.8e-9
SiC CVD	2.0	30	0.642	2.07	5.0e-7	3.2e-7	4.1e-10	2.8e-9
SiC CVD	2.0	0.50	0.642	0.03	8.5e-9	3.2e-7	4.1e-10	2.8e-9
SiC CVD	0.5	30	0.161	31	7.6e-6	4.8e-6	4.1e-10	4.2e-8
SiC CVD	0.5	0.50	0.161	0.56	1.4e-7	4.8e-6	4.1e-10	4.2e-8
SiC CVD	0.4	0.10	0.128	0.17	4.2e-8	7.4e-6	4.1e-10	6.5e-8
Silicon, ∅100mm	0.5	0.10	0.116	0.18	4.4e-8	3.4e-6	8.8e-10	5.9e-8
Silicon, ∅100mm	0.5	0.09	0.116	0.15	3.8e-8	3.4e-6	8.8e-10	5.9e-8

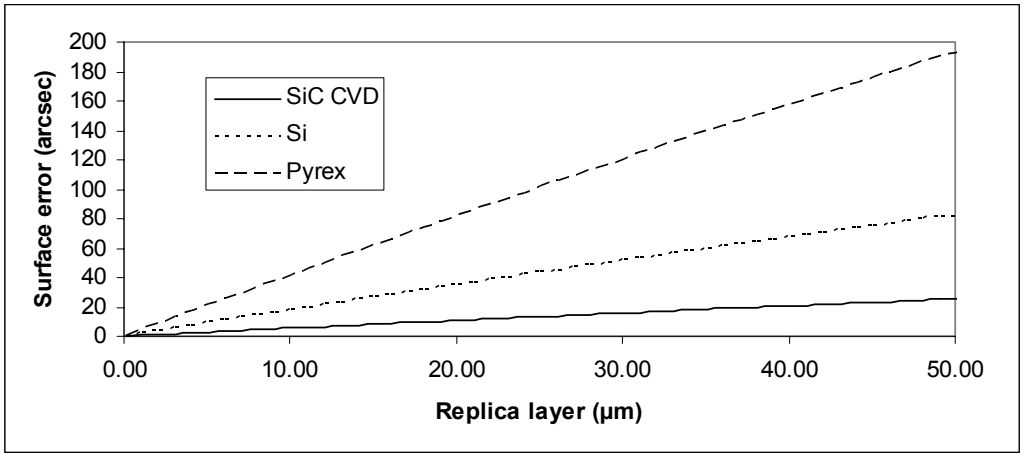

Figure 5. Surface error vs. replica layer thickness for ∅100mm, 0.5mm thick substrates

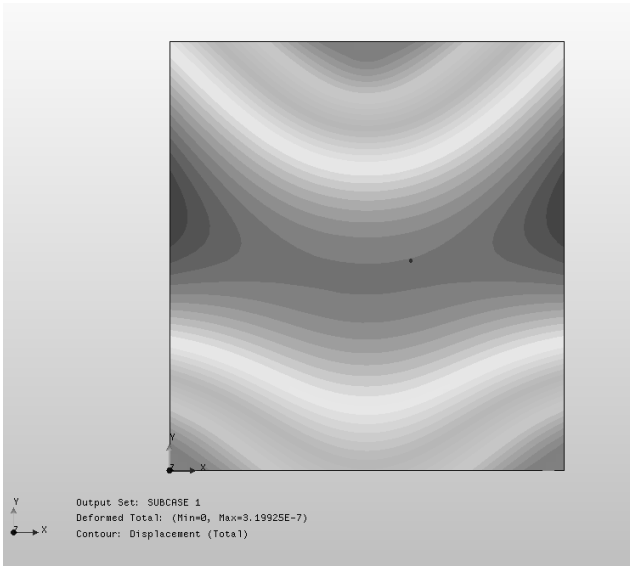

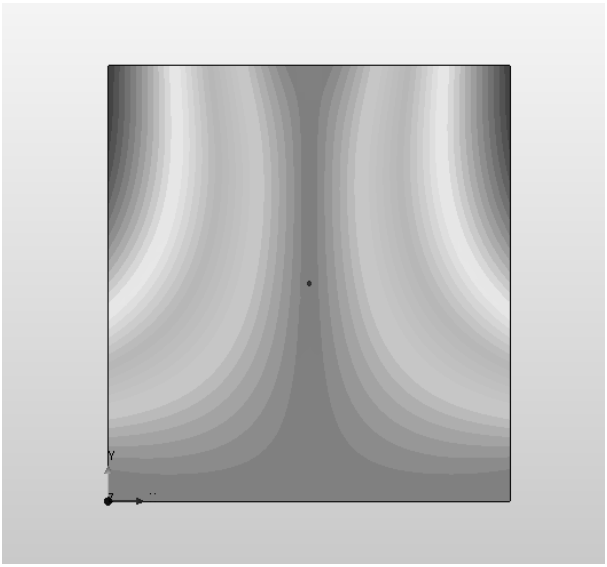

(a) 1g displacement in Z, 0.32μm (b) 1st mode – 1430 Hz

Figure 6. SiC substrate on a 5 point mount, 2mm thick

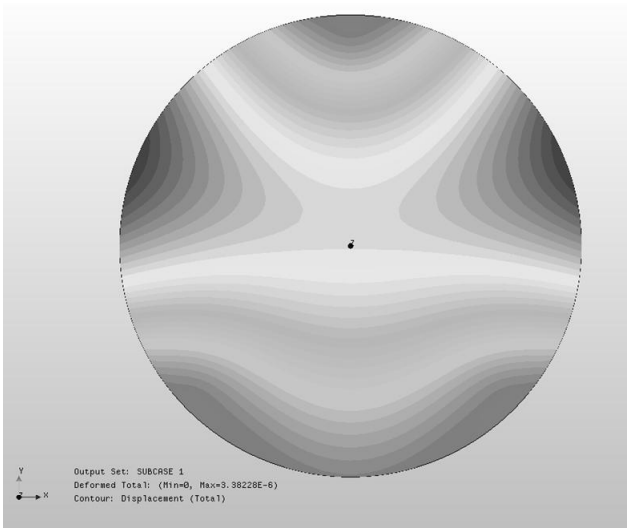

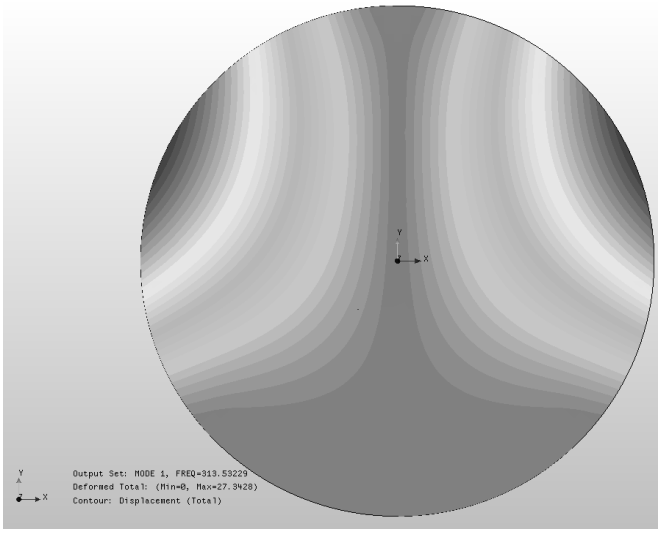

(a) 1g displacement in Z, 3.4μm (b) 1st mode – 314 Hz

Figure 7. Silicon wafer on a 3 point mount, 0.5mm thick

3.1. Flight environment analysis

The fundamental frequency of substrates is also predicted with a finite element model. See figures 6(b) and 7(b). This information is used in conjunction with equation 3 above to estimate a static equivalent launch load these gratings might expect to see in a flight application. Power spectral density in this calculation was taken from the vibration qualification test levels for the FUSE grating mount assemblies. FUSE was successfully launched on a Delta II rocket in 1998.[13] Since a flight mount has not yet been designed for gratings of this type, we assume a semi-kinematic restraint of three 4mm^2 areas over which the load is distributed. A Weibull statistical analysis is used to predict probability of fracture at launch with equation 5 below.[17] Table 5 compares the fracture probability of Pyrex, Silicon Carbide, and Silicon wafers for different substrate thicknesses. Here we see that fracture probability is largely influenced by Weibull material parameters rather than substrate thickness for thin optics.

$$P_{FW} = 1 - e^{\left(-\left(\frac{\sigma_a}{\sigma_0}\right)^m\right)} \quad (5)$$

where: P_{FW} = *probability of failure*
σ_a = *applied stress*
σ_0 = *Weibull scaling factor*
m = *Weibull modulus*

Table 5 Substrate f_n and Probability of Fracture

Substrate Type	Substrate Thickness	Fundamental Frequency (Hz)	Fracture Probability
Pyrex	2.0	631	1.6e-8
Pyrex	0.5	164	2.4e-9
SiC CVD	2.0	1430	1.2e-15
SiC CVD	0.5	371	< 1e-15
SiC CVD	0.4	298	< 1e-15
Silicon	0.5	314	1.4e-7

Gratings replicated by conventional means have substantial flight heritage and can be fabricated with low-outgassing resin to minimize potential molecular contamination, delamination or other forms of vacuum degradation. The replicated optics on FUSE have demonstrated consistent performance and reflectivity for several years on-orbit, suggesting these type replicas have good stability over time in vacuum. Gravity causes distortion in thin substrates, as shown in Table 4, and the effect of its release must be included in both surface figure and alignment budgets for flight applications. The survival temperature range for replicated gratings is limited by bi-metallic thermal stress between the substrate, replication layer, and reflection coating. The glass transition temperature of the replication resin must not be exceeded and may set the upper limit on survival temperature in some cases. For instance, the glass transition temperature, T_g, of the low-outgassing resin used in this analysis is at 85ºC. If it is exceeded the replication layer will soften, can relax or change with strain from the optic mount, and return to a glassy state with an altered optical surface. Bi-metallic strain also defines the operational temperature range on-orbit and allowable gradients for these thin gratings. Thermally induced surface error is driven by thermal expansion coefficient differences between the substrate, replication layer, reflection coating and mount.

SACRIFICIAL REPLICATION LAYER ONTO THIN SUBSTRATES

The University of Colorado has worked with NanoOpto Corporation to investigate the production of thin substrate gratings with a sacrificial replication layer.[18] The completed grating consists of a 0.5mm thick silicon wafer with a high density groove profile etched into its reflection coating. Figure 8 shows a SEM image of the (∅100mm) initial test grating with a 5000 line/mm groove profile etched into its 80nm thick gold reflection layer. NanoOpto uses a wet etching chemistry to maintain a smooth surface and no scattering is observed when it is used in an off-plane mount. Diffraction efficiency test results for a 5000g/mm NanoOpto parallel groove grating are shown in Figure 9. These efficiencies were taken using a x-ray spectrometer carbon line at 277eV. Off-plane performance of these gratings can be optimized in two ways: Adding blaze to the current sinusoidal groove profile as shown in Figure 10 will improve efficiency by diffracting light into fewer orders, and a radial groove pattern will make very high resolution optical designs possible. Although these upgrades have not yet been demonstrated, NanoOpto considers both achievable using their current technology. NanoOpto has also recently demonstrated the ability to produce these type gratings with parallel groove densities up to 10,000 lines/mm on a ∅4 inch wafer. Groove densities in this range present a great advantage for off-plane optical designs with resolution above 5000 ($\lambda/\Delta\lambda$).

The obvious advantage of these gratings is the absence of a polymer based replication layer and the surface distortion it causes. These gratings are also vacuum compatible and do not present a contamination risk. Thermal differences between the silicon substrate and reflection layer will still dictate the operational temperature range, but these gratings are otherwise similar to standard thickness flight optics with regard to the environment on-orbit.

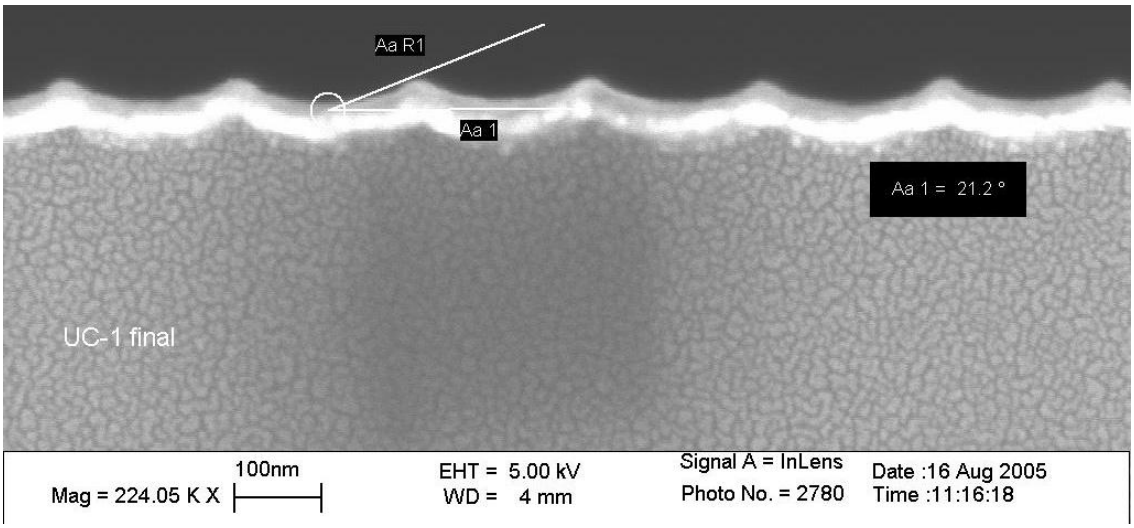

Figure 8. SEM cross section of etched reflection layer groove profile

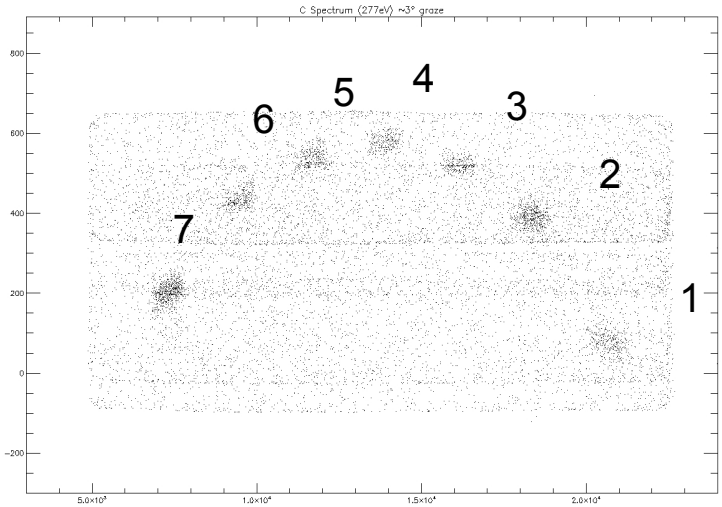

Spot	Absolute Efficiency
1	5.7%
2	5.9%
3	3.2%
4	4.7%
5	5.1%
6	4.1%
7	7.6%
Total	**36.3%**

Figure 9. Measured diffraction efficiency for sinusoidal NanoOpto grating, 5000 g/mm

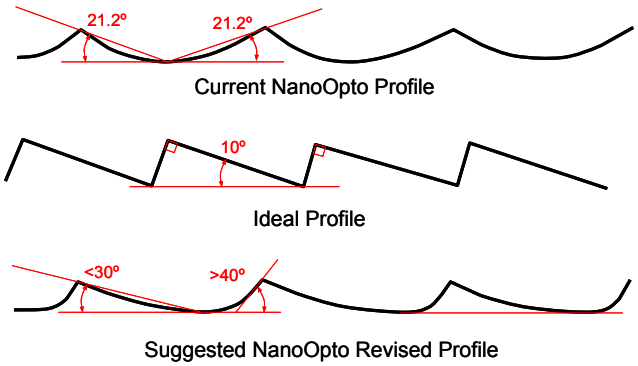

Figure 10. Current, ideal, and optimized line profile for NanoOpto grating

NANOIMPRINT LITHOGRAPHY (NIL) REPLICATION

The University of Colorado has not explored grating development using NIL replication techniques, but we include it in this study as an interesting and compelling option for thin substrate gratings. MIT's Space Nanotechnology Laboratory has worked in conjunction with Nanonex Corporation to investigate the development of NIL replicated gratings.[19] Parallel groove gratings were replicated onto silicon wafers by a variation of NIL replication used in the semiconductor industry. In this process, a 40mm x 40mm master with a 200nm groove period and 7º blaze angle is transferred onto a 0.5mm silicon wafer using a low-viscosity UV-curable liquid.[20] Groove features are well preserved with no obvious release damage. Residual stress in the cured polymer was estimated at 10MPa in an 85nm thick replication layer, and out-of-plane distortion was reported as <40nm on the backside of the wafer.[21] Diffraction efficiencies measured by Seely et al are excellent, and typical for well made gratings used in the off plane mount.[22] Overall these parallel groove gratings performed well, and as mentioned in the previous section, the development of a radial groove profile is desirable for optimal off-plane designs.

Gravitational effects are equivalent to those discussed for other thin substrate gratings, and thermal conditions are evaluated based on bimetallic effects as in the section on conventional replicas. The glass transition temperature (T_g) for common NIL polymers, such as Polymethyl methacrylate (PMMA), is about 60ºC. This is lower than T_g for existing low-outgassing resins used in conventional replication and may impose a lower limit on a survival temperature specification. Many existing NIL polymers are acrylic based, which is a material not generally rated as vacuum compatible. However, they are low-viscosity and construct very thin replication layers which reduce overall outgassing levels and potential molecular contamination. Regardless, technology transfer of NIL for space based applications will be greatly enhanced with the development of a low-viscosity, low outgassing polymer.

CONCLUSION

Several options for thin substrate gratings have been evaluated for an off-plane mount in a flight environment. We have shown that groove profiles replicated onto a thin substrate with polymers share a tendency to bend and cause optical surface error. Distortion is induced during the polymer curing process and is directly proportional to the replication layer thickness. Gratings made of stiff substrates with very thin or no replication layer will result in optimal surface figure. Test results demonstrate that smooth regular groove spacing results in good reflection efficiencies in an off plane mount. However, the addition of a blaze function improves performance by diffracting light into fewer orders and reducing required detector array size. Furthermore, radial groove patterns allow the advantage of high resolution optical designs in the off plane mount.

The effects of gravity on thin substrates and its release after launch need to be included in both surface figure and alignment tolerance budgets. Temperature changes and CTE difference between a substrate and reflection layer cause bimetallic bending and must also be included in the evaluation of figure and alignment. The glass transition temperature of a replication polymer is important and may set the upper limit on survival temperature. Replication polymers used in spaceflight applications need to be stable over time in a vacuum environment. Moreover, thin substrate gratings used in flight applications must be robust in a vibration environment and resist fracture.

In conclusion, we have shown there are several methods to produce gratings used in the type of closely packed arrays that are desirable in high energy astronomy. The larger challenge lies in mounting and alignment of these arrays for flight applications.

ACKNOWLEDGEMENTS

Thanks to Michael Kaiser for his contributions to design, assembly and test of electroformed gratings. This work was supported by NASA grants NNG04WC02G and NAG5-11850.

REFERENCES

1. W. Cash, "X-ray optics. 2: A technique for high resolution spectroscopy", *Applied Optics*, **30**, 1749-1759, 1991.
2. Randall L McEntaffer, Webster C Cash, Ann F Shipley, "Off-plane Gratings for Constellation-X," *Proc. Soc. Photo-Opt. Instr. Eng* **, 4851**, 549-556, 2002.
3. Webster Cash and Ann Shipley, "Off-plane grating mount tolerances for Constellation-X", *Soc. Photo-Opt. Instr. Eng*, **5488**, 335-340, 2004.
4. Randall L McEntaffer, Webster Cash, Ann Shipley, "A sounding rocket payload for X-ray observations of the Cygnus Loop", *Proc. Soc. Photo-Opt. Instr. Eng,* 2006.
5. Neviere, M., D. Maystre, W.R. Hunter, "On the use of classical and conical diffraction mountings for XUV gratings" 1978 *JOSA*, 68, 1106-1113.
6. W. Werner, "X-ray efficiencies of blazed gratings in extreme off-plane mountings" 1977, *Applied Optics*, 16, 2078- 2080.
7. Randall L McEntaffer, Webster Cash, Ann Shipley, "Sounding rocket payload development for X-ray observations of the Cygnus Loop," *Proc. Soc. Photo-Opt. Instr. Eng.,* **5900**, 2005.
8. Randall L. McEntaffer and Webster Cash, "High resolution x-ray spectroscopy of supernova remnants and the diffuse background", *Soc. Photo-Opt. Instr. Eng*, **5488**, 136-147, 2004.
9. W.P. Barnes, "Some effects of the aerospace thermal environment on high-acuity optical systems", *Applied Optics*, Vol. **5**, No. 5, 701, May 1966.
10. Anees Ahmad, *Handbook of Optomechanical Engineering*, CRC Press, 1997.
11. Ann Shipley, Randall McEntaffer, and Webster Cash, "Foil Reflection Grating Mount for Diffuse X-ray Spectroscopy", *Proc. Soc. Photo-Opt. Instr. Eng.,* **5877**, 2005.
12. James C. Green and Erik Wilkinson, "The design of the Far Ultraviolet Spectroscopic Explorer spectrograph", *Soc. Photo-Opt. Instr. Eng*, **2283**, 12-19, 1994.
13. Ann F. Shipley, James C. Green, and John P. Andrews, "The design and mounting of the gratings for the Far Ultraviolet Spectroscopic Explorer (FUSE)", **2542**, 185-196, 1995.
14. J.C. Green, "Cosmic Origins Spectrograph", *Proc. Soc. Photo-Opt. Instr. Eng*., **4013**, 352-359, 2000.
15. S. Osterman, E. Wilkinson, J.C. Green and K. Redman, "FUV grating performance for the Cosmic Origins Spectrograph", *Proc. Soc. Photo-Opt. Instr. Eng*, **4013**, 360-366, 2000.
16. Osterman, S.N., McEntaffer, R.L., Cash, W., Shipley, A., "Off-plane grating performance for Constellation-X", *Proc. Soc. Photo-Opt. Instr. Eng*. **5488**, 302-312, 2004.
17. Daniel C. Harris, *Materials for Infrared Windows and Domes,* SPIE Press, 1999.
18. Dr. Hubert Kostal, "Nano-optics: Changing the Rules For Optical System Design," NanoOpto Corporation White Paper #001, June 2003.
19. Chang et al., "High Fidelity Blazed Grating Replication using Nanoimprint Lithography", Journal of Vacuum Science & Technology B: Microelectronics and Nanometer Structures -- November 2004 -- Volume 22, Issue 6, pp. 3260-3264
20. C.-H. Chang, Fabrication of Extremely Smooth Blazed Diffraction Gratings, Master's thesis, Dept. of Mechanical Engineering, MIT, 2000.
21. R. K. Heilmann, M. Akilian, C.-H. Chang, C. G. Chen, C. R. Forest, C. Joo, J. C. Montoya, Y. Sun, J. You, and M. L. Schattenburg, "Advances in reflection grating technology for Constellation-X," in Optics for EUV, X-Ray, and Gamma-Ray Astronomy, O. Citterio and S. L. O'Dell, eds., Proc. SPIE 5168, pp. 271–282, 2004.
22. J. F. Seely et al, "Off-plane grazing incidence Constellation-X grating calibrations using polarized synchrotron radiation and PCGRATE code calculations *Proc. Soc. Photo-Opt. Instr. Eng***, 5900**, p. 73-80, 2005.